Mitigation of Vehicle Vibration Effect on Automotive MIMO Radar

O. Longman, I. Bilik, S. Villeval, and S. Shayovitz
General Motors, Advanced Technical Center - Israel
{oren.longman,igal.bilik,shahar.villeval}@gm.com;shachar.shay@gmail.com

***Abstract*—The high-resolution automotive radar is a key component in autonomous driving sensing suite. Vibration of the host vehicle degrades the automotive radar performance in terms of the maximal detection range and probability of false alarm. This work analyzes the effect of the vehicle vibration on the automotive multiple-input-multiple-output (MIMO) radar and proposes a method for its mitigation. The performance of the proposed approach is evaluated using collected radar measurements and measured vibration. It is shown that the proposed approach succeeds in vibration effect mitigation even with vibration model mismatch.**

I. Introduction

The automotive radar, along with cameras and lidars, is a key sensor enabling autonomous driving. Automotive radar is required to provide reliable information about the host vehicle surrounding and to report any object above the road surface obstructing the vehicle's motion. Moreover, automotive radar is required to provide imaging-like detail of the obstacle shape and therefore, has to posses high resolution in range, Doppler, azimuth and elevation.

The host vehicle mechanical vibration, induced by the engine operation and vehicle's interaction with the road surface, displace the radar position and as a result, shifts the radar echo phase [1]. The phase variation spread the returned energy across adjacent Doppler bins and reduce the energy at the Doppler bin that corresponds to the target's velocity. Resulting in probability of detection reduction. In addition, the phase vibration increase sidelobes in the Doppler domain and as a result degrade Doppler resolution and generate false alarms.

This work analyzes the host vehicle vibration effects on the automotive radar performance and proposes an approach for its mitigation. The vibration effect strongly depends on the radar frequency and integration duration. The proposed approach suggests first to estimate the vibration model from target detections. Next, the estimated model of the vibration is projected to all radar beams directions. Finally, the vibration effects are mitigated from the radar echoes and target detection is performed again.

The main novelty of this work is in a vibration mitigation approach that does not require auxiliary accelerometers measurements. This work adopts the simplified harmonic model in [1], and further demonstrates robustness to the vibrations modeling mismatch.

Performance of the proposed vibration mitigation approach is evaluated via simulations and by using accelerometer measurements of vehicle vibration and recorded radar echoes. In both tested scenarios, it is demonstrated that the proposed approach can mitigate vehicle vibration effects on the radar echoes and improve radar detection performance.

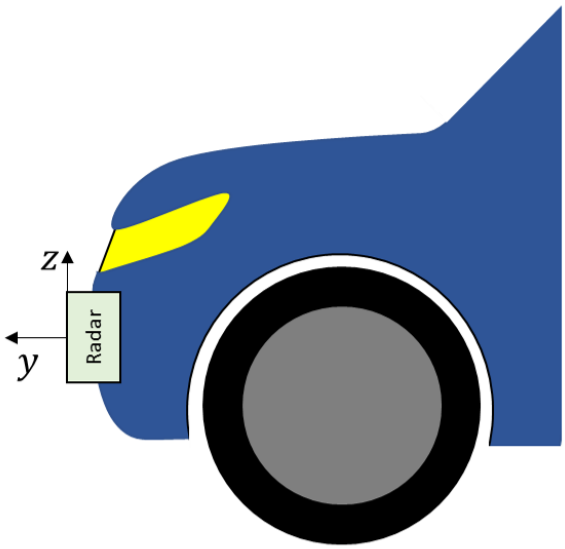

Fig. 1: Typical installation of the forward-looking automotive radar

The rest of this paper is organized as follows. The vehicle vibration model is presented in Section II. Section III demonstrates the vehicle vibration effect on the radar echoes. Section IV describes the proposed approach for vehicle vibration mitigation. The performance of the proposed vibration mitigation approach is evaluated in Section V via simulations and recorded radar measurements. The conclusions are summarized in Section VI.

II. Vehicle vibration model

The mechanical vehicle vibration was modeled in [1] as the following one-dimensional oscillatory motion along axis y in Fig. 1:

$$\begin{aligned} x(t) &= 0\ , \\ y(t) &= A_{vib}\sin(2\pi f_{vib}t + \varphi_{vib})\ , \\ z(t) &= 0\ , \end{aligned} \tag{1}$$

where A_{vib} is the vibration amplitude, f_{vib} is the vibration frequency and φ_{vib} is the phase. This model can be generalized

to any direction of vibration by axis rotation. For simplicity, this work assumes that the boresight of the automotive radar, mounted on the vehicle platform, and the vibration direction are aligned with the y axis.

III. Effect of Vehicle Vibration on Radar Echo

The displacement of the radar antenna along the y axis due to the host vehicle vibration effects the range between the radar and the target as follows:

$$\begin{aligned} R_{target} &= R_0 + D_0 t + R_{vib}(t) \\ &= R_0 + D_0 t + A_{vib}\sin(2\pi f_{vib} t + \varphi_{vib}) \ , \end{aligned} \tag{2}$$

where R_0 is the distance between the radar and the target, D_0 is the target radial velocity and R_{vib} is the antenna displacement due to the vehicle vibration. Since the vibration amplitude is significantly smaller than the range resolution, $A_{vib} \ll \Delta R$, the vibration effect on the range estimation is negligible.

For a linear frequency modulation (LFM) automotive radar with conventional processing in Fig. 2 [2]–[4], the transmitted signal (chirp) is:

$$s_{Tx}(t) = A_{Tx} e^{\pi j \alpha t^2} \ , \tag{3}$$

where α is the chirp slope and A_{Tx} is the amplitude of the transmitted signal. A series of transmitted chirps are reflected back from the target and processed according to the processing flow in Fig. 2, where the received echoes are first down-converted (de-chirped), sampled and applied a fast Fourier transform (FFT):

$$s_R[n] = A_R e^{2\pi j f_d t_n} \ , \tag{4}$$

where $f_d = \frac{2D_0}{\lambda}$ is the target Doppler frequency shift, n is the chirp index, λ is the signal wavelength, t_n is the nth chirp duration and A_R is the amplitude of the received radar echo. In the digital beamforming block in Fig. 2, the azimuth and elevation angles, θ_{az}, θ_{el}, of all range-spectrum peaks are obtained. The output of the beamformer is denoted as $s_{\text{beam}_i}[l, n]$, where i is the beam index and l is the range index. Next the Doppler-FFT is performed:

$$\begin{aligned} S_R[k] = \text{FFT}\{s_{\text{beam}_I}[n]\} &= \text{FFT}\{A_{\text{beam}_I} e^{2\pi j f_d t_n}\} \\ &= A_{\text{beam}_I}\delta[k - f_d] \ , \end{aligned} \tag{5}$$

where I is the beam index of the target direction and δ is the Kronecker delta function. The signal energy is accumulated to a single Doppler bin:

$$\max_k S_R[k] = \max_k |A_{\text{beam}_I}\delta[k - f_d]| = A_{\text{beam}_I} \ . \tag{6}$$

Notice that in the conventional processing flow of the automotive LFM radars, beamforming is performed only for peaks in the range-Doppler map [4]. The proposed vibration mitigation approach is directional, and thus, it is performed at the beam dimension after beamforming. Therefore, it is proposed to perform the beamforming for all peaks in the range spectrum, before Doppler-FFT.

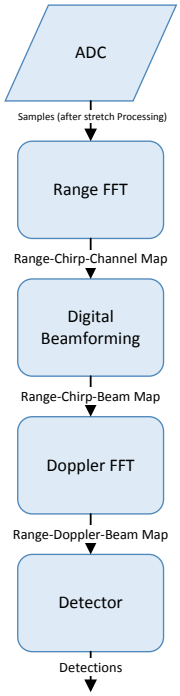

Fig. 2: Signal processing flow at the automotive LFM radar.

Considering the vibration model in (2), the radar echo is phase-shifted according to the range displacement in (2), and the radar echo after the range-FFT in (4) can be written as:

$$s_{vib}[n] = A_R e^{2\pi j (f_d t_n + \frac{A_{vib}}{\lambda}\sin(2\pi f_{vib} t_n + \varphi_{vib}))} \ . \tag{7}$$

The output of the Doppler-FFT in the presence of vibration is:

$$\begin{aligned} S_{vib}[k] = \text{FFT}\{s_{vib}[n]\} = \\ \text{FFT}\{A e^{2\pi j (f_d t_n + \frac{A_{vib}}{\lambda}\sin(2\pi f_{vib} t_n + \varphi_{vib}))}\} \ . \end{aligned} \tag{8}$$

Notice that in the presence of vibration, the range-Doppler spectrum in (8) is not a δ function. The energy is spread across multiple frequencies resulting in the energy loss in the target range-Doppler cell:

$$\max_k |S_{vib}[k]| < A_{\text{beam}_I} \tag{9}$$

This energy spread, as a result of the host vehicle vibration, degrades the signal-to-noise ratio (SNR) and therefore degrades the probability of detection. Moreover, energy spread across Doppler bins increases probability of false alarms. Notice that the vibration effect on the radar echo in the range-Doppler map increases as the signal wavelength decreases.

IV. Vibration Mitigation

The proposed method for vehicle vibration effect mitigation is summarized in Fig. 3. This approach consists of (a) vibration phase estimation, (b) cancellation of the estimated vibration effect, and (c) target corrected detection.

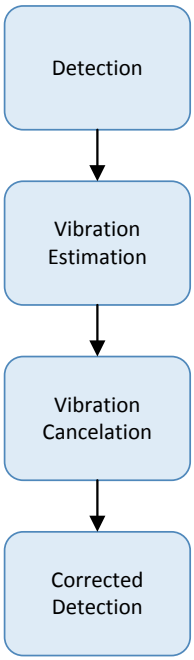

Fig. 3: Vibration mitigation process.

A. Vibration Estimation

The phase of s_{vib} in (7) is:

$$\varphi[n] = \tan^{-1}\frac{Im\{s_{vib}[n]\}}{Re\{s_{vib}[n]\}} = 2\pi(f_d t_n + \frac{A_{vib}}{\lambda}\sin(2\pi f_{vib} t_n + \varphi_{vib}))\ , \tag{10}$$

where the target Doppler, f_d, is defined by the relative motion between the target and the host vehicle. The proposed method considers detections from M stationary (zero-Doppler) objects (e.g. road clutter) to estimate the vibration phase in the received radar echo as follows:

$$y_m[n] = \varphi_m[n] - 2\pi f_h t_n\ , \tag{11}$$

where $f_h = \frac{2V_h}{\lambda}$ is the host vehicle Doppler, V_h is the host vehicle radial velocity and m is the detection index.

The estimation of the global vibration effect in (1) on the radar echo can be obtained from multiple spatially-distributed detections of stationary objects, as follows:

$$\hat{y}_{\text{glob}}[n] = \frac{1}{M}\sum_{n=1}^{N}\hat{y}_{\text{glob}_m}[n] \tag{12}$$

where for the mth detection:

$$\hat{y}_{\text{glob}_m}[n] = \frac{y_m[n]}{\cos(\theta_{az_m})\cos(\theta_{el_m})}\ , \tag{13}$$

where θ_{az_m} and θ_{el_m} are the estimated azimuth and elevation angles of the mth detection.

B. Vibration Cancellation

First, the vibration estimation is projected to all beam-directions in the range-chirp-beam maps:

$$y_{\text{beam}_i}[n] = \hat{y}_{\text{glob}}[n]\cos(\theta_{az_i})\cos(\theta_{el_i})\ , \forall i\ , \tag{14}$$

where θ_{az_i} and θ_{el_i} are the azimuth and elevation angles of the ith beam. Next, the vibration effects are canceled by correcting each chirp phase:

$$\hat{s}_{\text{beam}_i}[k,n] = s_{\text{beam}_i}[k,n]e^{-j\hat{y}_{\text{beam}_i}[n]},\quad \forall i\ . \tag{15}$$

Notice that this stage requires the range-chirp-beam map. Therefore, the conventional automotive radar signal processing flow is modified and the order of the beamformer and the Doppler FFT is switched. The corrected detection is performed on the corrected data $\hat{s}_{\text{beam}_i}[k,n]$ in (15), where the vibration effect is mitigated. Notice that the proposed vibration effect mitigation process can be extended to non stationary targets using an iterative process.

V. Performance Evaluation

Performance of the proposed vibration mitigation method is evaluated in this section. Both simulated and measured vibration are first used to evaluate their effect on the recorded radar echoes, and next, the capability of the proposed vibration mitigation approach is evaluated. The radar echoes from a point-target (corner reflector) were collected using the 77GHz automotive radar [4].

A. Vibration Simulation

First, the vibration in (1) with amplitude of 1mm and frequency of 50Hz is simulated. Fig. 4 shows the Doppler spectrum of the recorded radar echoes with and without the simulated vibration. Notice that the vibration spreads the Doppler spectrum. Phase estimation of the radar echoes and the corresponding estimation error are shown in Fig. 5.

Next, the proposed vibration mitigation approach is applied on the recorded radar echo with simulated vibration. The signal at the output of the vibration mitigation process is shown in Fig. 6. Notice that the vibration effect is completely mitigated in this scenario.

B. Measured Vibration

Fig. 7 shows the accelerometer-measured automotive radar displacements along y axis due to the vehicle vibration, when driving at the speed of $20\frac{m}{s}$ on a subtly uneven surface.

The collected measurements of the 77GHz automotive radar are ~~range~~ shifted according to this displacement. Fig. 8 shows the Doppler spectrum of the recorded radar signal with and without vibration effects.

Notice, that the vibration effect introduces an additional phase into the radar echoes, which is a function of the wavelength, λ:

$$\Delta\Phi = \frac{2\pi\Delta R}{\lambda} \tag{16}$$

where ΔR is the range displacement due to vibration, and $\Delta\Phi$ is the additional vibration phase. Therefore, the significance of the vibration effects on the radar echoes increases

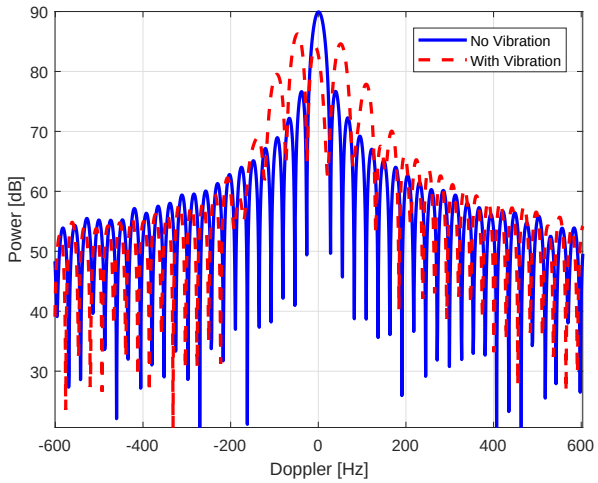

Fig. 4: Doppler spectrum of recorded radar echo with and without simulated vibration.

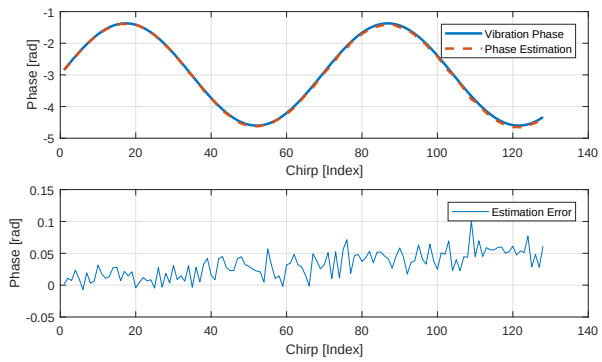

Fig. 5: Simulated vibration phase and its estimation.

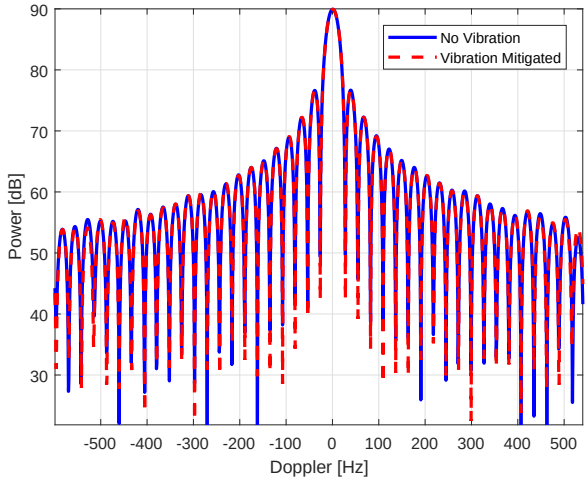

Fig. 6: Doppler spectrum of recorded radar signal without vibration and with mitigated vibration.

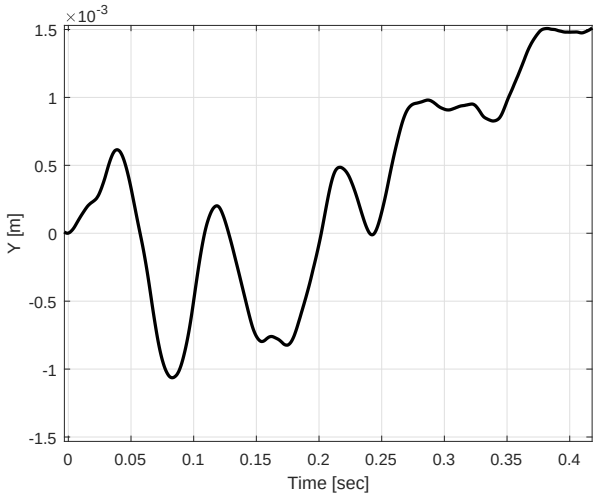

Fig. 7: Accelerometer-measured displacement of the on-vehicle mounted automotive radar due to vibration along y axis while driving at the speed of $20\frac{m}{s}$

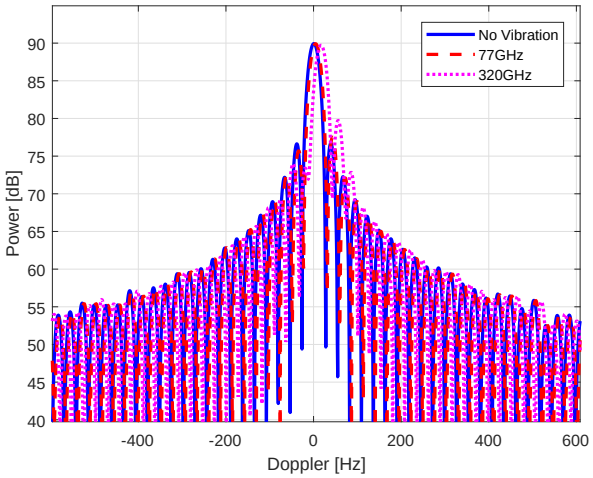

Fig. 8: Doppler spectrum of recorded radar signal with TOT of 36msec without vibration and with vibration effects at 77GHz and extrapolated for 320 GHz.

with the increasing frequency ($f = \frac{c}{\lambda}$). The requirements for higher angular resolution of automotive radars motivates their implementation at a higher frequency, and thus, future automotive radars are expected to operated at 320GHz [5]–[7]. The Doppler spectrum of the radar echoes with vibration at 320GHz is simulated in Fig. 8. Notice its increased spread upon comparison with the Doppler spectrum of the radar at 77GHz.

Further, notice that the vibration effect on the radar echoes depends on the time-on-target (TOT). Current automotive radars consider TOT of 40msec, however, long coherent integration time is desirable for future automotive radars [8]–[10]. Radar measurements with longer TOT incorporate larger phase change induced by the vibration. Fig. 9 shows the Doppler spectrum of the automotive radar signal with and without vibration when TOT is 110msec. By comparing the Doppler

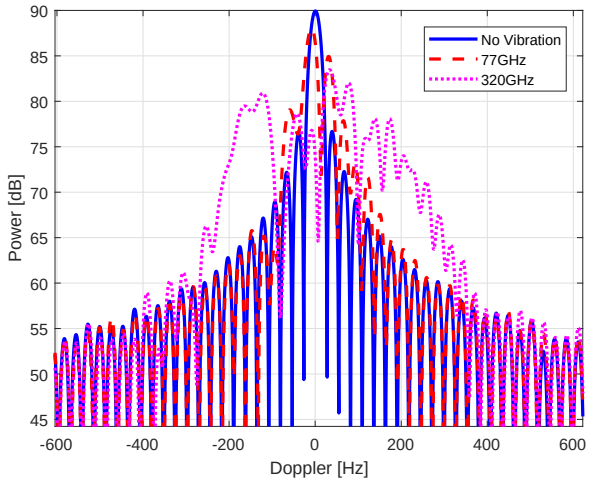

Fig. 9: Doppler spectrum of recorded radar signal with TOT of 110msec without vibration and with vibration effects at 77GHz and extrapolated for 320 GHz.

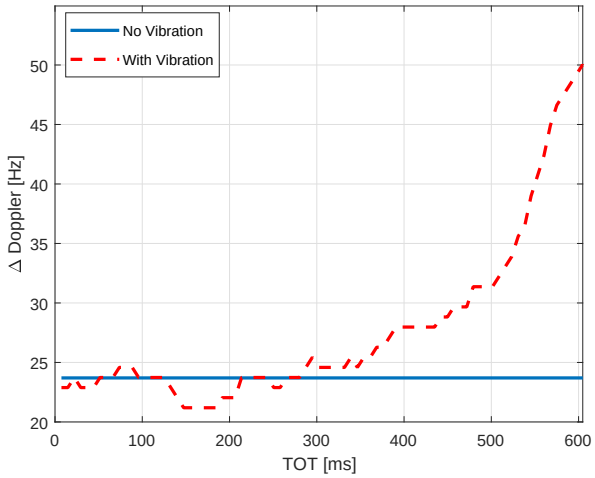

Fig. 10: Doppler resolution of the automotive radar with vibration at the 3dB points of the Doppler spectrum main lobe as a function of the TOT

spectrum in Fig. 9 with Fig. 8 a significant increase in the Doppler spread sidelobe levels, is noticeable.

Operation of fast-LFM automotive radars in dense urban environment, which is characterized by multiple closely-spaced distributed targets, strongly depends on the high-Doppler resolution. Fig. 10 shows the vibration effect on the Doppler resolution of automotive radar, which is defined at the 3dB points of the Doppler spectrum main lobe, as a function of TOT. Notice the significant Doppler resolution loss of the 77GHz automotive radar with TOT beyond 300msec.

Fig. 11 shows the energy loss in the main peak of the radar Doppler spectrum due to vibration effects, as a function of TOT. This effect of the Doppler spectrum spread results in lower SNR and degraded probability of detection.

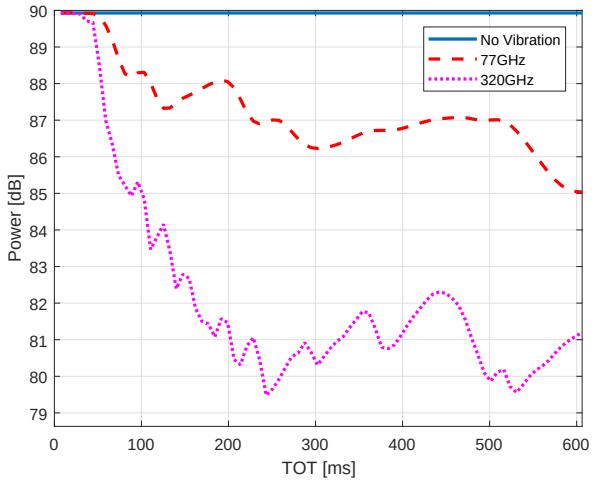

Fig. 11: Power of the Doppler spectrum main lobe in the presence of vibration as a function of TOT.

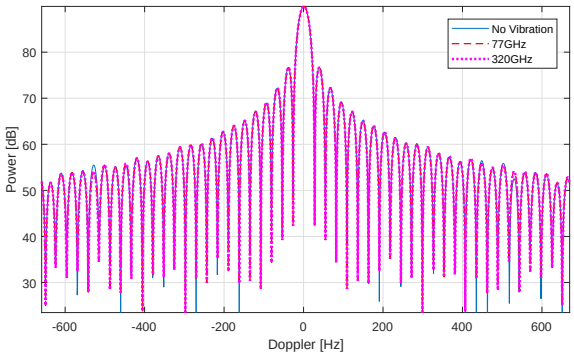

Fig. 12: Doppler spectrum of recorded radar signal at TOT of 110msec without vibration and with mitigated vibration.

C. Vibration Mitigation

The performance of the proposed vibration mitigation approach is evaluated in this subsection using radar measurements at operation frequencies of 77GHz, and extrapolated for 320GHz, with added displacement according to measured vibration in Fig. 7 and TOT of 110msec. Fig. 12 shows the Doppler spectrum of the radar echo with vibration when using the proposed vibration mitigation approach. Comparison between the Doppler spectrum in Fig. 12 with Fig. 9, demonstrates that the proposed approach succeed to mitigate the vibration effect on the radar echoes. Notice that the harmonic model of vibration in (1) does not accurately represent measured vibration. However, the proposed approach succeed to mitigate vibration effect on the radar echoes and thus provides robustness to the model mismatch.

VI. Conclusions

Effects of vehicle vibration on the automotive radar echoes were analyzed in this work. It was shown that vehicle vibration spreads the radar echo Doppler spectrum, and results in Doppler resolution loss and decreased signal-to-noise ratio. It

was also demonstrated that the vibration effects on the radar echoes increase with increasing time-on-target and operation frequency. Next, the vibration effects mitigation approach was proposed and its performance was evaluated via simulations and by using recorded vibration and radar measurements. The capability of the proposed approach to mitigate the vibration effects on the radar echoes was demonstrated and its robustness was shown in a scenario with vibration model mismatch. Where, the presented vehicle vibration model, a first order sinusoidal model, did not match the recorded vibration.

REFERENCES

[1] F. Hau, F. Baumgärtner, and M. Vossiek, "Influence of vibrations on the signals of automotive integrated radar sensors," in *Microwaves for Intelligent Mobility (ICMIM), 2017 IEEE MTT-S International Conference on*, pp. 159–162, 2017.

[2] M. Murad, I. Bilik, M. Friesen, J. Nickolaou, J. Salinger, K. Geary, and J. Colburn, "Requirements for next generation automotive radars," in *Radar Conference (RADAR), 2013 IEEE*, pp. 1–6, 2013.

[3] I. Bilik, O. Bialer, S. Villeval, H. Sharifi, K. Kona, M. Pan, D. Persechini, M. Musni, and K. Geary, "Automotive MIMO radar for urban environments," in *Radar Conference (RadarConf), 2016 IEEE*, pp. 1–6, 2016.

[4] I. Bilik, S. Villeval, D. Brodeski, H. Ringel, O. Longman, P. Goswami, C. Y. B. Kumar, S. Rao, P. Swami, A. Jain, A. Kumar, S. Ram, K. Chitnis, Y. Dutt, A. Dubey, and S. Liu, "Automotive multi-mode cascaded radar data processing embedded system," in *2018 IEEE Radar Conference (RadarConf18)*, pp. 0372–0376, April 2018.

[5] A. Stove, "Potential applications for low-Tera-Hertz radar," in *2015 16th International Radar Symposium (IRS)*, pp. 191–196, June 2015.

[6] D. R. Vizard, M. Gashinova, E. G. Hoare, and M. Cherniakov, "Low THz automotive radar developments employing 300600 GHz frequency extenders," in *2015 16th International Radar Symposium (IRS)*, pp. 209–214, June 2015.

[7] R. Appleby and R. N. Anderton, "Millimeter-Wave and Submillimeter-Wave Imaging for Security and Surveillance," *Proceedings of the IEEE*, vol. 95, pp. 1683–1690, Aug 2007.

[8] D. Wang, C. Lin, Q. Bao, and Z. Chen, "Long-time coherent integration method for high-speed target detection using frequency agile radar," *Electronics Letters*, vol. 52, no. 11, pp. 960–962, 2016.

[9] X. Chen, J. Guan, N. Liu, and Y. He, "Maneuvering Target Detection via Radon-Fractional Fourier Transform-Based Long-Time Coherent Integration," *IEEE Transactions on Signal Processing*, vol. 62, pp. 939–953, Feb 2014.

[10] X. Rao, H. Tao, J. Xie, J. Su, and W. Li, "Long-time coherent integration detection of weak manoeuvring target via integration algorithm, improved axis rotation discrete chirp-fourier transform," *IET Radar, Sonar Navigation*, vol. 9, no. 7, pp. 917–926, 2015.